Frictiotaxis underlies adhesion-independent durotaxis

Adam Shellard[1,*], Peter A. E. Hampshire[2,3], Namid R. Stillman[1], Christina Dix[4], Richard Thorogate[5], Albane Imbert[3], Guillaume Charras[1,5], Ricard Alert[2,3,*], Roberto Mayor[1,6,*]

[1]*Department of Cell and Developmental Biology, University College London, Gower Street, London, WC1E 6BT, UK*
[2]*Max Planck Institute for the Physics of Complex Systems, Nöthnitzerst. 38, 01187, Dresden, Germany*
[3]*Center for Systems Biology Dresden, Pfotenhauerst. 108, 01307, Dresden, Germany*
[4]*The Francis Crick Institute, 1 Midland Road, London, NW1 1AT, UK*
[5]*London Centre for Nanotechnology, University College London, London, WC1H 0AH, UK*
[6]*Center for Integrative Biology, Faculty of Sciences, Universidad Mayor, Santiago, Chile*

Abstract

Cells move directionally along gradients of substrate stiffness, a process called durotaxis. The current consensus is that durotaxis relies on cell-substrate focal adhesions to transmit forces that drive directed motion. Such a mechanism implies that focal adhesion-independent durotaxis is impossible, although this assumption has never been tested. Here, we show that confined cells can perform durotaxis despite lacking strong or specific adhesions. We show that the mechanism of this adhesion-independent durotaxis is that stiffer substrates offer higher friction. We develop a physical model that predicts that non-adherent cells polarize and migrate towards regions of higher friction — a process that we call frictiotaxis. We demonstrate frictiotaxis in experiments by showing that cells migrate up a friction gradient even when stiffness is uniform. Our results broaden the potential of durotaxis to guide any cell that contacts a substrate and reveal a new mode of directed migration based on friction, with implications for immune and cancer cells, which commonly move with non-specific interactions.

***Correspondence: adam.shellard.13@ucl.ac.uk; ralert@pks.mpg.de; r.mayor@ucl.ac.uk**

The ability of cells to migrate following environmental gradients underlies many aspects of development, homeostasis and disease (*1, 2*). Cells follow gradients in the stiffness of their substrate, a process called durotaxis that has been demonstrated in multiple cell types *in vitro* and *in vivo* (*3-7*). The prevailing mechanistic view of durotaxis involves the cells' actomyosin machinery producing contractile forces that pull on the underlying substrate through focal adhesions. These pulling forces then bias cell motion in one direction, typically toward the stiffer substrate (*7-10*). These physical models are supported by experimental evidence, and an essential component of all of them is strong cell-substrate adhesions. It is thus believed that cells lacking adhesions must be incapable of sensing stiffness gradients. Whether cells lacking cell-matrix adhesions can respond to mechanical gradients is widely acknowledged as a vital question (*11-14*) that has been unaddressed. Its importance is highlighted by the fact that adhesion-independent motility is a fundamental mode of migration, classically exhibited by various cancer and immune cells, but which can be triggered in practically any cell type by providing 3D confinement (*15, 16*).

Part of the challenge in addressing whether cells migrating without adhesions are capable of responding to stiffness gradients, or indeed the role of substrate stiffness in the context of 3D adhesion-independent motility in general, lies in the technical challenge of fabricating confined cellular environments of tuneable stiffness that are necessary to study adhesion-independent migration (*14*). Adhesion-independent motility has commonly been studied using the 'under agarose assay' in which cells emigrate from a free region into confinement between agarose and glass. However, this method is unable to differentiate between the effect of confinement and the effect of compression since

cells must deform their substrate to move. A newer method uses microchannels fabricated with polydimethylsiloxane (PDMS). However, this material exhibits stiffness in the MPa range, far from physiologically relevant levels of most tissues, and offers little ability to tune rigidity. We developed a novel and easy-to-use method in which mobile and deformable cells spontaneously migrate into and within agarose-surrounded preformed microchannels (Fig. 1A). Fabricating microchannels with agarose offers the potential to investigate cells within substrates of physiologically relevant stiffnesses (*17*). The stiffness of the microchannel is tuned by the concentration of agarose (Fig. 1B). The dimensions of the channel are determined by a PDMS mould that provides reliable confinement irrespective of microchannel dimensions (Fig. 1, C and D and fig. S1, A to C) and is unaffected by the stiffness of the substrate (Fig. 1, E to G and fig. S1, D and E). Fluorospheres did not show directed motion within microchannels, confirming that pressure-driven fluid flow was not a factor in this setup (fig. S1, F and G). Moreover, stiffness gradients can be created by combining solutions with different agarose concentrations together during microchannel assembly (Fig. 1, H and I).

To test our setup as a valid means of assaying confined non-adherent cellular motility, we used a non-adherent subline of Walker 256 carcinosarcoma (henceforth Walker) cells as a well-validated model of a cell type that moves without using specific substrate adhesions and without focal adhesions (*18, 19*). Walker cells introduced into the agarose microchannel setup exhibited classical amoeboid motion characterised by bleb-based rather than lamellipodium-based motility (Fig. 1J, fig. S2, A and B, and movie S1), fast movement (Fig. 1K) and lack of focal adhesions (Fig. 1, L and M).

To directly address whether cells are capable of undergoing durotaxis in an adhesion-independent manner, agarose microchannels were fabricated to have either uniform stiffness or a stiffness gradient (Fig. 1, H and I and Fig. 2A). We tracked migratory cells that entered regions of the microchannel which exhibited either uniform or graded stiffness. Cells entering substrate of uniform stiffness had a moderate tendency to repolarise and move back,

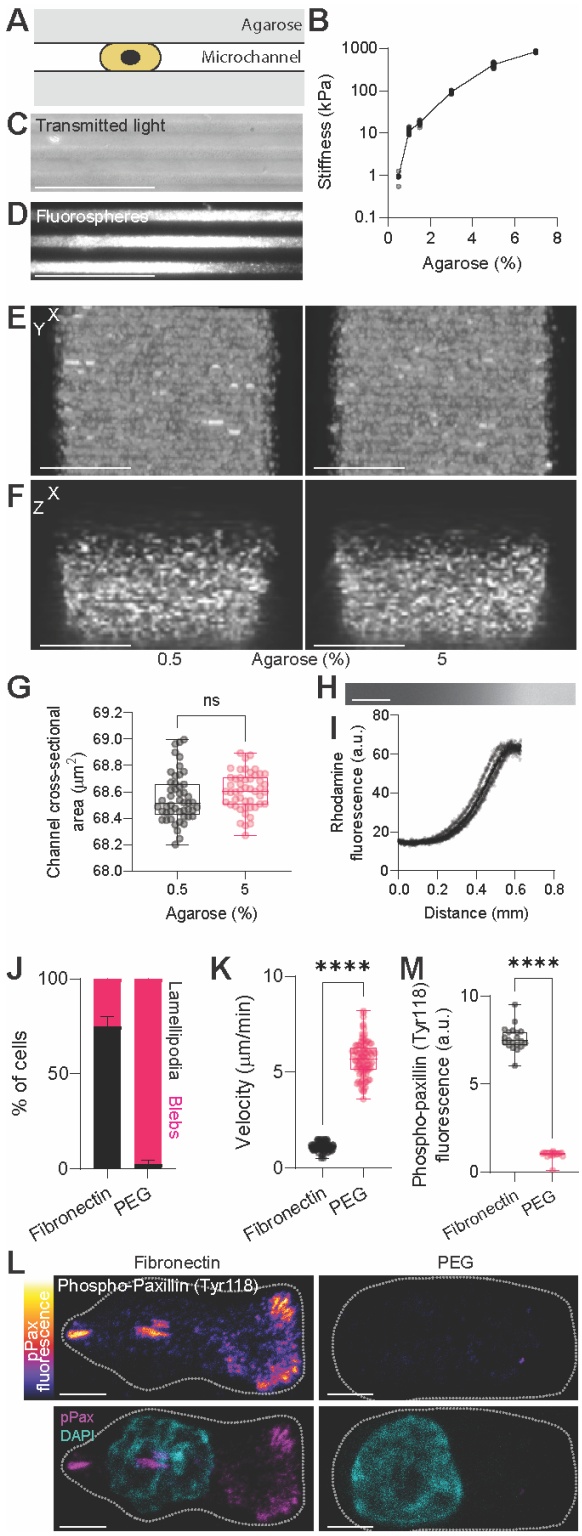

Figure 1. A microchannel system with tuneable stiffness and dimensions. (**A**) A diagram of the microchannel assay. Microchannels of dimensions determined by a photopatterned Si wafter determines the geometry of the setup and is surrounded by agarose which determines substrate stiffness. (**B**) Stiffness measurements (mean ± s.d.) by nanoindentation of gels of different agarose concentration. Grey dots represent individual data points. n = 25 cells. (**C and D**) Agarose channels (C) filled with 0.2 μm fluorospheres (D). Scale bar, 100 μm. (**E to G**) Agarose microchannels (E and F; 0.5%, left; 5%, right) filled with 0.2 μm fluorospheres and imaged from below (E, maximum projection) and side-on (F). Channel cross-sectional area quantified (G).

Scale bar, 5 µm. (**H and I**) A stiffness gradient visualized by immersing rhodamine dextran dye into one of the agarose solutions prior to subsequent diffusion and solidification (H) and quantification of the dye fluorescence over the gradient axis (I). Scale bar, 100 µm. Grey dots represent individual data points. $n = 5$ gels. (**J**) Quantification of lamellipodia and blebs by cells in adhesive (fibronectin) and non-adhesive (PEG) regimes. $N = 3$ experimental repeats. (**K**) Velocity of cells migrating within agarose microchannels with fibronectin or PEG substrate. (**L and M**) Immunostaining phospho-paxillin (Tyr118) in Walker cells within agarose channels (L) and quantification (M) in which the underlying glass is coated with either PLL-g-PEG or fibronectin. Dotted white line represents the cell outline. Scale bar, 5 µm. $n = 100$ cells (K, M).

whereas cells entering a stiffness gradient were characterised by much higher persistence as they migrated toward the stiff substrate (Fig. 2, B to E, and movie S2). Like Walker cells, HL60 neutrophil-like cells, a cell type with a well-described amoeboid behaviour (*20*), also exhibited preferred motion toward stiffer substrate (fig. S3). Together, these results reveal adhesion-independent durotaxis may be a generalisable phenomenon.

Given that amoeboid cells lack focal adhesions, it was unclear how these cells were able to durotax. We hypothesized that regions of higher stiffness may offer higher friction, which arises from non-specific molecular interactions between the cell membrane and the channel walls (*19*). We also hypothesised that, in the absence of active forces pulling the substrate, this passive friction would cause amoeboid cells to undergo durotaxis.

We investigated this hypothesis through a physical model of amoeboid motility which treats the actomyosin network in the cell cortex as an active gel (*12, 15, 16, 19, 21-25*). In this model, myosin-generated contractility triggers an instability whereby the gel concentrates towards one side, which becomes the cell rear (Fig. 3A). This concentration profile drives retrograde actomyosin flow, which propels the cell forward. In the absence of external gradients, symmetry is broken spontaneously. The cell can thus move either left or right (Fig. 3A), consistent with our experimental observations of repolarisation events in uniform channels (Fig. 2C-D).

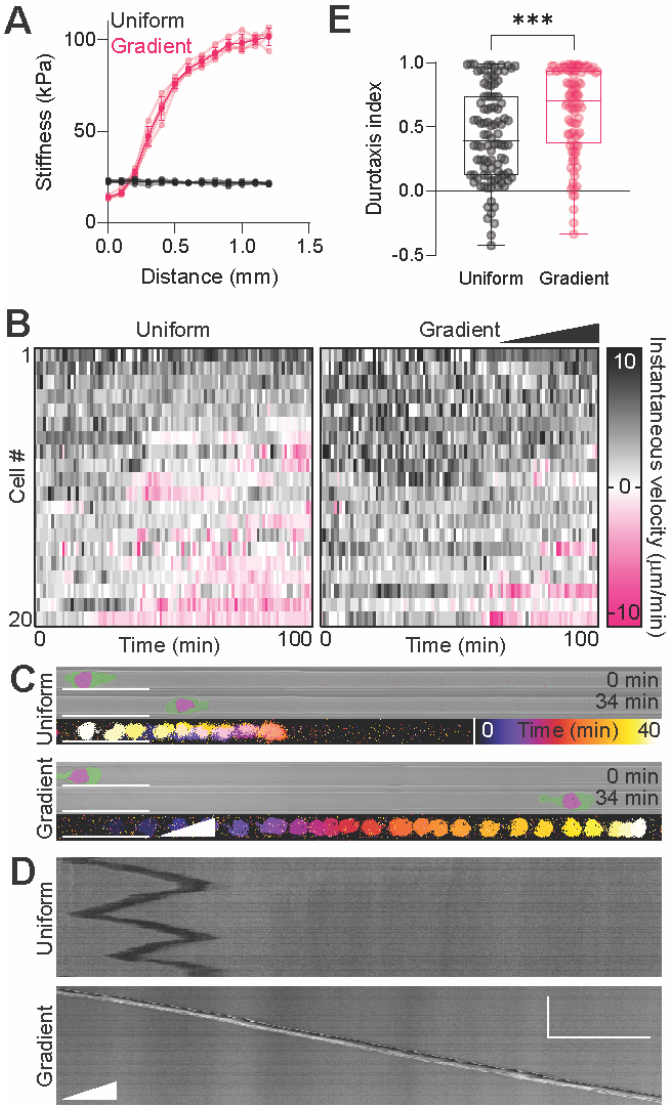

Figure 2. Adhesion-independent durotaxis of Walker cells. (**A**) Stiffness measurements (mean ± s.d.) from nanoindentation of uniform (black) and gradient (pink) microchannels. Opaque dots and lines represent mean; translucent dots and lines are raw data. $n = 5$ gels each. (**B**) Heat maps of the instantaneous velocity representative cells migrating within microchannels of uniform or graded stiffness. $n = 20$ representative cells each. Each row represents a different cell. The x-axis represents time, with each box representing 1 min for a total of 100 min. Each heat map is ordered such that cells migrating forward (black) are at the top, and cells migrating backwards (pink) are at the bottom. (**C**) Example pictures of cells at an earlier (top panels) and later (middle panels) time point, and temporal colour-coded projected tracks (bottom panels). Cells are tracked by a nuclear marker and membrane is pseudocoloured. Scale bar, 50 µm. (**D**) Kymographs of the cells shown in (C). Scale bar, 50 µm (horizontal), 50 min (vertical). (**E**) Quantification of durotaxis. $n = 100$ cells.

Within the framework of this model, we next asked what would happen if the gel were exposed to an external friction gradient. We show that, in the model, a friction gradient can break the symmetry and yield motion towards regions of higher friction.

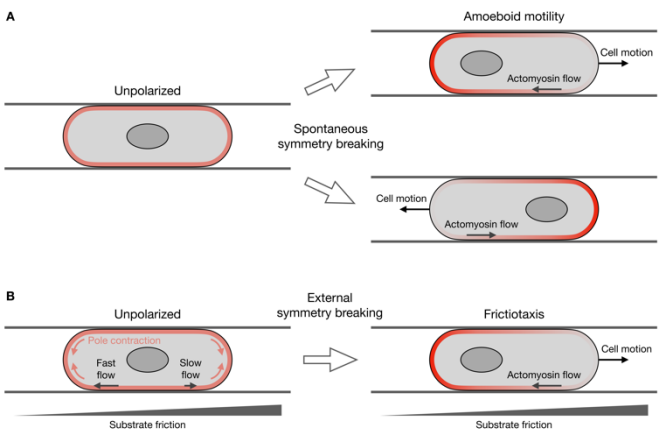

Figure 3. Model of frictiotaxis. (A) In the absence of external gradients, unpolarized cells break symmetry spontaneously and display amoeboid motility either left or right. (B) On a friction gradient, contractile stresses from the poles produce faster cortical flows on the lower-friction side. These flows break the symmetry and accumulate actomyosin towards the low-friction side, which drives frictiotaxis, that is directed cell migration towards higher friction.

Starting from an unpolarized state with uniform gel concentration, contractile stresses from the cell poles generate faster cortex flows in low-friction areas. These flows concentrate the gel towards the low-friction side, which thus becomes the cell rear (Fig. 3B).

To demonstrate this mechanism of symmetry breaking, we considered force balance for the actomyosin gel:

$$\xi \phi v = \frac{\mathrm{d}\sigma}{\mathrm{d}x}. \tag{1}$$

The left-hand side represents gel-substrate friction, which is proportional to the coefficient $\xi(x)$, the volume fraction $\phi(x)$ of the gel, and its velocity $v(x)$ with respect to the substrate. The right-hand side represents the forces generated within the gel. These forces arise from gradients of the gel stress $\sigma = \sigma_\mathrm{a} + \sigma_\mathrm{v} - \Pi$, which includes contributions from active contractility, $\sigma_\mathrm{a} = \zeta\phi$, gel viscosity $\sigma_\mathrm{v} = \eta\phi\, \mathrm{d}v/\mathrm{d}x$, and osmotic pressure $\Pi = \alpha(\phi - \phi_0)^3 - \gamma\, \mathrm{d}^2\phi/\mathrm{d}x^2$ (*21*). Here, ζ, η, α, and γ are material parameters described in more detail in (*21*) and in the SI, and ϕ_0 is the equilibrium volume fraction of the gel.

Because the cell poles are not subject to substrate friction, they undergo the contractile instability earlier and faster than the rest of the gel. The resulting pole contraction pulls in gel from the central region of the cell (Fig. 3B). In the central region, the gel starts in the unpolarized state with uniform gel concentration $\phi(x) = \phi_0$, for which the force balance Eq. (1) reduces to

$$\xi v = \eta \frac{\mathrm{d}^2 v}{\mathrm{d}x^2}. \tag{2}$$

To capture the mechanism of symmetry breaking, we solve this force balance close to the two ends of the central region, which are subject to a stress σ_pole arising from pole contraction and have different friction coefficients ξ_- and ξ_+, with $\xi_- < \xi_+$. Thus, we obtain the velocities of the two ends, v_+ and v_- (SI):

$$v_\pm = \pm \frac{\sigma_\mathrm{pole}}{\sqrt{\eta\, \xi_\pm}}. \tag{3}$$

As illustrated in Fig. 3B, this result shows that the gel flows faster towards the pole in the low-friction region, which leads to gel accumulation towards that side and subsequent cell motion towards high-friction regions.

Overall, our theory predicts a mode of cell migration guided by friction gradients (Fig. 3B), which we call frictiotaxis. These results suggest that cells without strong focal adhesions perform durotaxis by exploiting gradients in friction rather than stiffness variations.

To test this idea in experiments, we first probed the relationship between stiffness and friction by performing lateral force microscopy (LFM) on the agarose microchannels across the stiffness range in which we observed durotaxis. LFM measures the torsional deformation of the micro-mechanical cantilever of an atomic force microscope during contact mode, enabling the measurement of frictional properties. We found that, in accordance with our hypothesis, stiffer substrates exhibited higher friction forces (Fig. 4A).

If amoeboid durotaxis is based on friction, it should be impaired if the channel walls are passivated with polyethylene glycol (PEG), which has been shown to provide low-friction substrates (*19, 26*).

Additionally, cells should be capable of directed migration when stiffness is uniform, but friction is graded.

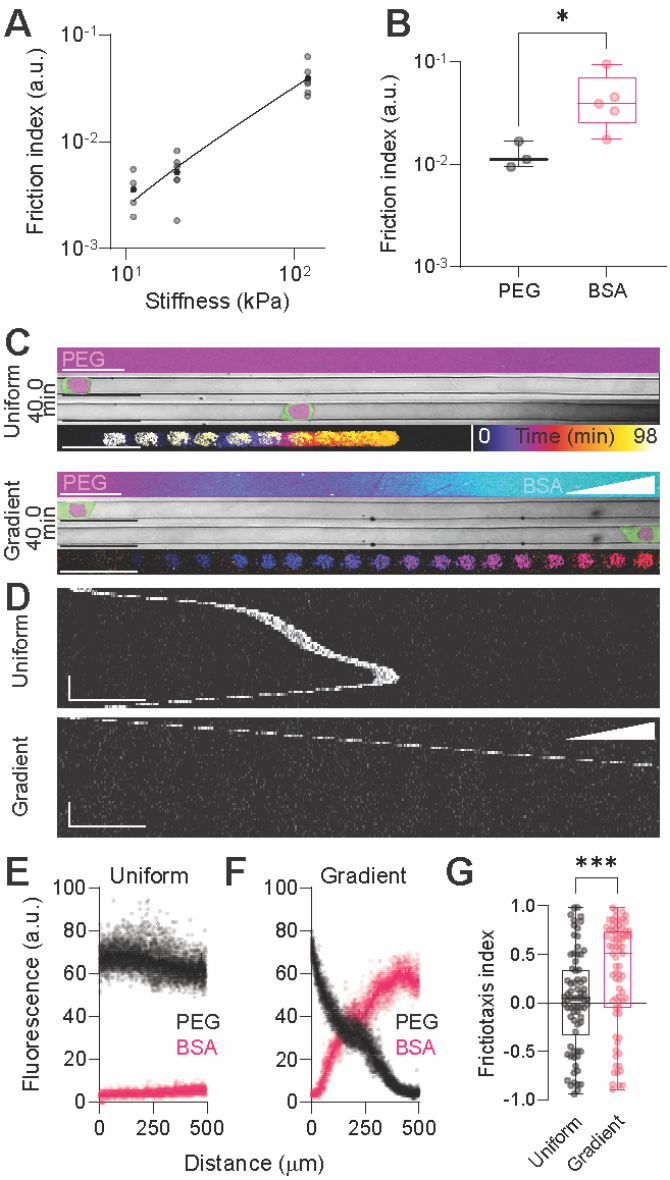

Figure 4. Friction-driven directed migration. (**A**) Friction index versus stiffness in the gels; $n = 4$ (*in vitro*, at 11 kPa); $n = 6$ (*in vitro*, other stiffness values). (**B**) Friction of PEG- or BSA-treated glass; $n = 3$ (PEG); $n = 5$ (BSA). (**C and D**) Images of PLL-g-PEG/FITC and BSA-Alexa647 micropatterning (top panels, C), earlier and later time points of examples cells (middle panels, C), temporal colour-coded projected tracks (bottom panels, C), and kymographs (D). Cells were tracked by a nuclear marker and membrane was pseudocoloured. Scale bar, 50 µm. Vertical scale bar (D), 10 min. (**E and F**) Quantification of micropatterned PEG and BSA in the microchannel setup; $n = 10$ (PEG); $n = 9$ (BSA). (**G**) Durotaxis index; $n = 74$.

To test the first prediction, we employed a previously described method in which agarose is coupled to proteins after the surface is activated with cyanogen bromide, enabling functional interactions between the cell and the coated surface (*27, 28*). As a proof of principle, cells adhered strongly to fibronectin-coated agarose gels (fig. S4A). We thus coated agarose microchannels exhibiting a stiffness gradient with PLL-g-PEG (fig. S4, B and C). Cells migrating through such channels had impaired durotaxis, compared to controls (fig. S4, D and E). Thus, durotaxis is abrogated by lack of friction despite the presence of a stiffness gradient.

To address whether gradients in friction are sufficient to guide cell migration in the absence of adhesions, we generated gradients in friction by micropatterning gradients of bovine serum albumin (BSA), which provides high friction, and PEG, which provides low friction (*19*), onto glass and within PDMS microchannel substrate (Fig. 4, C to E and fig. S5), such that regions without BSA contained PEG. By performing LFM, we validated that BSA-coated regions provided higher friction than PEG-coated regions (Fig. 4B), which supports previous evidence (*19*). We observed cells moving toward areas of higher friction when they migrated in these channels, as opposed to randomly directed motion when friction was uniform (Fig. 4, C and F, and movie S3). Motion guided by friction gradients was previously conceptualized (*29*) and demonstrated in magnetic colloidal particles (*30*). Here, our experimental data confirm that cells perform frictiotaxis, and they suggest that this mode of directed migration provides the mechanism for adhesion-independent durotaxis.

Altogether, our study contributes to the growing field questioning how the physical environment modulates adhesion-independent migration (*23, 31, 32*). Our results reveal that strong and specific adhesions are redundant for durotaxis thanks to non-specific friction forces, which enable preferential movement toward stiffer substrates because stiffness and friction are correlated. In practice, different tissues may exhibit different stiffness-friction relationships, thus affecting cell response. Although cells performing amoeboid migration might have weak adhesions, the mechanism of directed motion that we reveal is entirely based on friction. Accordingly, our model includes no adhesion, i.e., no resistance to normal pulling forces, but just friction that opposes cell-substrate sliding.

Modulating only one physical variable, in this case stiffness, to investigate cell behaviour is a major challenge. Despite establishing the dominant role of friction, we cannot rule out that differential substrate deformation contributes to adhesion-independent

durotaxis. In this study, we used microchannels that were larger than the nucleus, because amoeboid cells use the nucleus as a mechanical gauge in path-making decisions (*33*). We also chose to use pre-formed paths, rather than an 'under agarose assay', to rule out the role of compression on the cells, since under compressive regimes, cells must physically deform their surroundings to move, which is more difficult when the substrate is stiffer (*31*). Whether cell compression and other physical input can act as guidance cues for adhesion-independent cell motility remains an open question. Notably, however, geometric patterns can guide adhesion-independent motility (*23, 34*).

Finally, whether frictiotaxis and amoeboid durotaxis are physiologically relevant in the complex *in vivo* environment, especially considering chemotactic signals are extremely potent drivers of directional cell migration, is also unknown. A promising candidate are immune cells, which often need to traverse tissues of high density to reach target sites. Adhesion-independent durotaxis could contribute significantly to this type of directed migration.

1. A. Shellard, R. Mayor, All Roads Lead to Directional Cell Migration. *Trends in Cell Biology* **30**, 852-868 (2020).
2. S. SenGupta, C. A. Parent, J. E. Bear, The principles of directed cell migration. *Nature Reviews Molecular Cell Biology* **22**, 529-547 (2021).
3. A. Shellard, R. Mayor, Durotaxis: The Hard Path from In Vitro to In Vivo. *Developmental Cell* **56**, 227-239 (2021).
4. C. M. Lo, H. B. Wang, M. Dembo, Y. L. Wang, Cell movement is guided by the rigidity of the substrate. *Biophysical Journal* **79**, 144-152 (2000).
5. A. Shellard, R. Mayor, Collective durotaxis along a self-generated stiffness gradient in vivo. *Nature* **600**, 690-694 (2021).
6. D. E. Koser *et al.*, Mechanosensing is critical for axon growth in the developing brain. *Nature Neuroscience* **19**, 1592-1598 (2016).
7. R. Sunyer *et al.*, Collective cell durotaxis emerges from long-range intercellular force transmission. *Science* **353**, 1157-1161 (2016).
8. R. Alert, J. Casademunt, Role of Substrate Stiffness in Tissue Spreading: Wetting Transition and Tissue Durotaxis. *Langmuir* **35**, 7571-7577 (2019).
9. A. Isomursu *et al.*, Directed cell migration towards softer environments. *Nature Materials* **21**, 1081-1090 (2022).
10. M. E. Pallares *et al.*, Stiffness-dependent active wetting enables optimal collective cell durotaxis. *Nature Physics* **19**, 279-289 (2023).
11. K. M. Yamada, M. Sixt, Mechanisms of 3D cell migration. *Nature Reviews Molecular Cell Biology* **20**, 738-752 (2019).
12. E. K. Paluch, I. M. Aspalter, M. Sixt, Focal Adhesion-Independent Cell Migration. *Annual Review of Cell and Developmental Biology,* **32**, 469-490 (2016).
13. H. D. Moreau, M. Piel, R. Voituriez, A. M. Lennon-Dumenil, Integrating Physical and Molecular Insights on Immune Cell Migration. *Trends in Immunology* **39**, 632-643 (2018).
14. D. L. Bodor, W. Ponisch, R. G. Endres, E. K. Paluch, Of Cell Shapes and Motion: The Physical Basis of Animal Cell Migration. *Developmental Cell* **52**, 550-562 (2020).
15. Y. J. Liu *et al.*, Confinement and Low Adhesion Induce Fast Amoeboid Migration of Slow Mesenchymal Cells. *Cell* **160**, 659-672 (2015).
16. V. Ruprecht *et al.*, Cortical Contractility Triggers a Stochastic Switch to Fast Amoeboid Cell Motility. *Cell* **160**, 673-685 (2015).
17. C. F. Guimaraes, L. Gasperini, A. P. Marques, R. L. Reis, The stiffness of living tissues and its implications for tissue engineering. *Nature Reviews Materials* **5**, 351-370 (2020).
18. M. Bergert, S. D. Chandradoss, R. A. Desai, E. Paluch, Cell mechanics control rapid transitions between blebs and lamellipodia during migration. *Proceedings of the National Academy of Sciences of the United States of America* **109**, 14434-14439 (2012).
19. M. Bergert *et al.*, Force transmission during adhesion-independent migration. *Nature Cell Biology* **17**, 524-529 (2015).
20. K. Wilson *et al.*, Mechanisms of leading edge protrusion in interstitial migration. *Nature Communications* **4**, (2013).
21. A. C. Callan-Jones, R. Voituriez, Active gel model of amoeboid cell motility. *New Journal of Physics* **15** (2013).
22. R. J. Hawkins *et al.*, Spontaneous Contractility-Mediated Cortical Flow Generates Cell Migration in Three-Dimensional Environments. *Biophysical Journal* **101**, 1041-1045 (2011).
23. A. Reversat *et al.*, Cellular locomotion using environmental topography. *Nature* **582**, 582-585 (2020).
24. A. C. Callan-Jones, R. Voituriez, Actin flows in cell migration: from locomotion and polarity to trajectories. *Current Opinion in Cell Biology* **38**, 12-17 (2016).
25. A. Callan-Jones, Self-organization in amoeboid motility. *Frontiers in Cell and Developmental Biology* **10** (2022).
26. S. Byun *et al.*, Characterizing deformability and surface friction of cancer cells. *Proceedings of the National Academy of Sciences of the United States of America* **110**, 7580-7585 (2013).
27. J. Carlsson, D. Gabel, E. Larsson, J. Ponten, B. Westermark, Protein-coated agarose surfaces for attachment of cells. *In Vitro-Journal of the Tissue Culture Association* **15**, 844-850 (1979).
28. J. Porath, R. Axen, S. Ernback, Chemical Coupling of Proteins to Agarose. *Nature* **215**, 1491-1492 (1967).
29. A. E. Carlsson, Mechanisms of cell propulsion by active stresses. *New Journal of Physics* **13** (2011).
30. J. P. Steimel, J. L. Aragones, A. Alexander-Katz, Artificial Tribotactic Microscopic Walkers: Walking Based on Friction Gradients. *Physical Review Letters* **113** (2014).
31. F. Gaertner *et al.*, WASp triggers mechanosensitive actin patches to facilitate immune cell migration in dense tissues. *Developmental Cell* **57**, 47-62 (2022).
32. R. M. Brunetti *et al.*, WASP integrates substrate topology and cell polarity to guide neutrophil migration. *Journal of Cell Biology* **221** (2021).

33. J. Renkawitz *et al.*, Nuclear positioning facilitates amoeboid migration along the path of least resistance. *Nature* **568**, 546-550 (2019).
34. M. Le Berre *et al.*, Geometric Friction Directs Cell Migration. *Physical Review Letters* **111** (2013).
35. Y. Ding, G. K. Xu, G. F. Wang, On the determination of elastic moduli of cells by AFM based indentation. *Scientific Reports* **7** (2017).
36. M. Rubinstein, R. H. Colby, *Polymer Physics*. (Oxford University Press, Oxford, 2003).
37. M. Doi, *Introduction to Polymer Physics*. (Oxford University Press, Oxford, 1995).

Acknowledgements

We thank E. Paluch for gifting us Walker 256 carcinosarcoma cells, L. Alvizi for advice with tissue culture and J. Hartmann for assistance with stitching. We thank P. Saez and M. Piel for advice about PDMS and microchannels. We thank Alveole and Cairn for providing access to the PRIMO, as well as P. March for access to the PRIMO at the University of Manchester. P.H. and R.A. thank A. Callan-Jones, P. Haas, and J. Neipel for discussions on the model.

Funding

Medical Research Council (MR/S007792/1).

Biotechnology and Biological Services Research Council (M008517).

Biotechnology and Biological Services Research Council (BB/T013044).

Wellcome Trust (102489/Z/13/Z).

Author contributions

A.S. conceived the project, performed the experiments, and analysed the experimental data. R.A. and P.H. developed the physical model and derived the explanation of frictiotaxis. N.S. contributed to conceptualisation of the model and performed AFM with R.T. with assistance from G.C. G.C. provided conceptual and technical advice, especially with AFM and tissue culture. A.S and C.D. generated the silicon wafers in A.I.'s laboratory. A.S., R.M. and R.A. wrote and edited the manuscript. All authors commented on the manuscript.

Competing interests

The authors declare that they have no competing interests.

Data and materials availability

All data are available in the main text or the supplementary materials.